

Vortex behaviour of an unbaffled surface aerator

Achanta Ramakrishna Rao, Bimlesh Kumar*, Ajey Kumar Patel

Department of Civil Engineering, Indian Institute of Technology, Guwahati, India

*Corresponding author, e-mail: bimk@civil.iisc.ernet.in

Received 27 Mar 2008

Accepted 31 May 2009

ABSTRACT: Agitating liquids in an unbaffled surface aeration tank leads to the formation of a vortex in the region of the impeller shaft. The types and characteristics of the vortex govern the process phenomena of a surface aeration tank. In the present work, experimental results and empirical correlations have been obtained to relate the vortex depth to a number of physical factors. Experiments have been carried out on geometrically similar surface aeration systems, so that the present results can be simulated in the field conditions. The critical speed at which the vortex reaches the impeller has been estimated. It is found that around critical speed, there is an observable change in mass transfer characteristics, power used for mixing, and radius of the forced vortex zone. Equations for predicting vortex depth in geometrically similar surface aeration tanks have also been developed.

KEYWORDS: surface aeration tank, power consumption, mixing power, Rankine vortex, energy cost

INTRODUCTION

Aeration is an essential process in the majority of wastewater treatment plants and accounts for the largest fraction of the plant energy costs, ranging from 45% to 75% of the plant energy expenditure¹. The rising costs of electricity and other energy forms are now causing engineers and their clients to reevaluate the design of aeration systems. The economics of an aeration system, particularly operating costs, are contributing much more heavily to the system selection².

Aeration systems transfer oxygen into a liquid media by either diffusing gas through a gas-liquid interface, or dissolving gas into the liquid solution using a semi-permeable membrane. Many different types of aeration systems have been developed over the years to improve the energy efficiency of the oxygen transfer process; they can be classified as (1) surface or mechanical aeration methods, which increase interfacial area by spraying water droplets into the air, (2) diffused aeration methods, which release air bubbles beneath the surface of the water, and (3) combined or turbine aeration methods, which introduce large air bubbles into the water and reduce their sizes mechanically.

Surface aerators are a popular choice of aeration system because of their inherent simplicity, reliability, and their competitive rate of oxygen transfer per unit of power input under actual aeration conditions. Surface aerators are the most common reactors that are used almost universally for gas dispersion and re-

actions in biochemical, fermentation, and wastewater treatment industries³⁻⁵.

Surface aeration will be defined as the aeration or oxygen transfer that takes place in the gas-liquid interface when the liquid is agitated, without the sparging of air. For effective aeration in a surface aerator, the impeller is located near the free liquid surface. The important functions of surface aerators include oxygen transfer and liquid phase mixing to ensure oxygen availability in all parts of the contactor.

Although baffled configurations are found in most industrial stirred vessels, there are numerous applications where unbaffled tanks are used. Unbaffled vessels consume less power than the baffled vessels⁶. In free-surface unbaffled tanks, the central vortex, usually regarded as a drawback, may be desirable in a number of situations⁷. For example, the central vortex is effective in drawing down floating solid particles or in removing gas bubbles from the liquid, thus reducing foam formation. The absence of baffles in a vessel typically results in the generation of a central vortex and a swirling flow⁸. Also, baffles are usually omitted in the case of very viscous fluids where, as a result of giving rise to dead zones, they may actually worsen the mixer performance. In such cases vortex formation is inhibited by the low rotational speed and by the high friction on the cylindrical wall⁹. Unbaffled tanks are also advisable in crystallizers, where the presence of baffles may promote particle attrition¹⁰. Finally, unbaffled tanks give rise to higher fluid-particle mass transfer rates for a given power consumption, which

may be desirable in a number of processes¹¹.

Mass transfer operations of a surface aeration system are greatly affected by the vortex behaviour. Vortex shape and depth are dependent on the agitation rate, the liquid medium viscosity, and tank geometry. For example, the depth of the impeller below the liquid surface will cause air entrainment if the impeller is close to the surface. The entrainment decreases the further away the bottom of the vortex gets from the agitator¹². Vortex formation can greatly affect the power consumption. In the design and scale-up of surface aeration systems, it is always important to estimate the critical impeller speed at which vortex reaches the impeller.

In the present work, an attempt is made to determine the important parameters that influence the vortex depth in unbaffled surface aeration tanks. Thus, the objectives of this work are (1) to investigate the effect of vortex formation on process phenomena such as mass transfer rates, power consumption, and critical impeller speed and (2) to develop an equation for vortex depth in geometrical similar unbaffled surface aeration systems so that the present results can be rescaled for the field application.

THEORETICAL CONSIDERATIONS

A typical surface aerator is shown in Fig. 1. The various dimensions of the aerator are: D (tank diameter), H (water depth), h (distance between the horizontal bottom of the tank and the top of the blades), d (diameter of the rotor), h_v (the depth of the vortex) and Z_0 (distance between the horizontal bottom of the

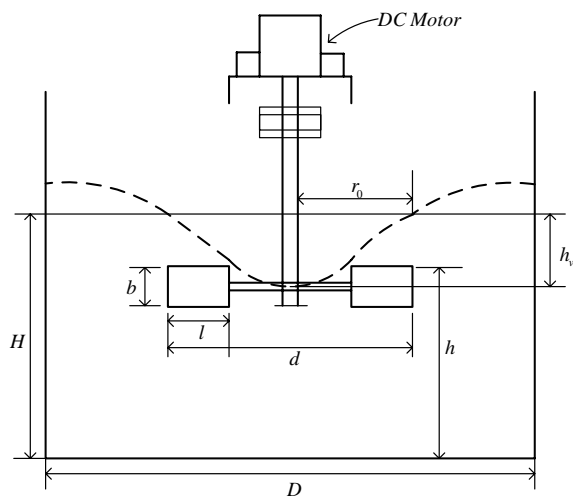


Fig. 1 Schematic diagram of the unbaffled aerator with vortex geometry.

tank and centre of the vortex). We used a type of disk turbine rotor. As a result of its high local shear and suitability for dispersion processes, the disk turbine is one of the most commonly used mixers for gas-liquid mass transfer in the processes of chemical industries, particularly in the cases of low or intermediate gassing rates¹³. The rotor is fitted with six flat blades in a symmetrical manner. The rotor shaft is connected to a DC motor to rotate the rotor at the desired speed (N).

A vortex is produced as a result of centrifugal force acting on the rotating liquid. When the impeller is rotating, a vortex will develop on the surface of the liquid. Many investigators^{7-9,11} have found that there are two types of motion in the flow of a liquid agitated by a mixer. A zone with a constant angular velocity (vortex zone) is formed in the central part of the vessel, and a zone where the peripheral velocity of the liquid decreases according to the hyperbolic law (irrotational zone) is formed in the remaining part. The so-called vortex zone is supposed to exist inside a hypothetical cylinder of critical radius r_0 ($0 \leq r \leq r_0$), in the centre of vessel, which is assumed to rotate as a solid body with an angular velocity equal to that of the rotor⁹. The aforementioned type of vortex is called Rankine vortex⁹. In this geometry the vorticity is uniformly distributed in a cylinder of radius r_0 with a central line as its axis. The tangential component of velocity (v_t) is continuous in r but a break appears at r_0 . Assuming that the axial flow is very small and therefore negligible in comparison with the tangential liquid flow and there is no contribution from the continuity equation⁸, the r and z components of the equation of motion can be expressed as^{7,14}:

$$\frac{\partial p}{\partial r} = \frac{v_t^2}{rg}, \quad \frac{\partial p}{\partial z} = -\rho g. \tag{1}$$

In the Nagata model of the Rankine vortex¹⁵:

$$v_t = \begin{cases} \omega r, & r \leq r_0, \\ \omega r_0^2/r, & r > r_0, \end{cases} \tag{2}$$

where ω is the angular velocity of the liquid. By integrating (1) and (2) over the forced and free vortex regions, Nagata⁹ has obtained the following equation for determining r_0 :

$$\frac{(H - Z_0)g}{(\omega D)^2} = \left(\frac{r_0}{D}\right)^2 - 4\left(\frac{r_0}{D}\right)^4 \left(\frac{3}{4} + \ln\left(\frac{D}{2r_0}\right)\right). \tag{3}$$

Another important aspect is to find N_{crit} , the critical impeller speed at which gas is entrained as the result of the gas/liquid interface reaching the impeller¹⁶. Operation at $N > N_{crit}$ will result in

increased transfer from gas to liquid and a change in impeller power consumption and mixing characteristics. Hence it is imperative to know the critical speed in a surface aeration system.

The whole system can be analysed in terms of energy balance. Referring to Fig. 1, between the top edge of the vortex and the centre of the vortex there is difference in potential energy. To maintain this potential energy difference between the two points, there should be a continuous conversion of kinetic energy (imparted by the impeller rotation) into potential energy. The most convenient term to represent this kinetic energy is the one related to the speed at the tip of the rotating blades¹⁷. The energy balance is expressed as

$$V_d \rho g = k(\pi^2 d^2 N^2 \rho) / 2. \quad (4)$$

Alternatively it can be written as

$$\frac{V_d}{d} = k Fr \quad (5)$$

where Fr is the impeller Froude number and equals $N^2 d/g$. The value of k can be obtained by plotting the observations of vortex depth and Froude number of the surface aeration tanks. The value of k can be also be derived by re-arranging (3) in the form of (5)¹⁶. Then

$$k = \left(\frac{2\pi r_0}{d}\right)^2 \left[1 - \left(\frac{2r_0}{D}\right)^2 \left(\frac{3}{4} + \ln\left(\frac{D}{2r_0}\right)\right)\right]. \quad (6)$$

On the basis of experimental observations, previous studies^{15,16,18,19} also report that (3) applies for an impeller operating in the turbulent mixing region. Hence if k is known, N_{crit} can be obtained by re-arranging (5) to give

$$N_{crit} = \sqrt{\frac{V_d g}{k d^2}}. \quad (7)$$

In general, (3) can also be expressed as

$$V_d = f(N, d, D, \nu, g, H - h) \quad (8)$$

where ν is the kinematic viscosity. In dimensionless form, V_d/d is a function of just Fr and the Galileo number, $Ga \equiv Re^2/Fr$, where Re is impeller Reynolds number and equals Nd^2/ν . This relationship (the relation of vortex depth with Ga and Fr) helps when scaling up the surface aeration tanks^{19,20}.

MEASUREMENT OF PHYSICAL PARAMETERS

Two sizes of unbaffled circular tanks of cross-sectional areas A equal to 1.0 m^2 and 0.52 m^2 were

tested under laboratory conditions. The following conditions of geometric similarity as suggested by Udaya et al²¹ were maintained in all the surface aerators:

$$\begin{aligned} \sqrt{A}/d &= 2.88, & H/d &= 1.0, & l/d &= 0.3, \\ b/d &= 0.24, & h/d &= 0.94, \end{aligned}$$

where b and l are the the blade width and length, respectively. Detailed discussion on the measurement of mass transfer coefficients and power consumption has been given in Refs. 6, 22. Two-film theory²³ has been used to measure the mass transfer coefficient. According to two-film theory, the oxygen transfer coefficient, $K_L a_T$, where subscript T is the temperature expressed in °C, is given by

$$K_L a_T = \frac{1}{t} (\ln(C_s - C_0) - \ln(C_s - C_t)), \quad (9)$$

where C_0 , C_t , and C_s are, respectively, the dissolved oxygen (DO) concentrations at the start, at time t , and after a very long time (its saturation value). The value of $K_L a_T$ can be obtained from slope of a plot of $\ln(C_s - C_t)$ against t . The value of $K_L a_T$ was corrected for a temperature other than the standard temperature of 20 °C by using the van't Hoff-Arrhenius equation²⁴. The effective power (P) available at the shaft was calculated from²⁵:

$$P = I_2 V_2 - I_1 V_1 - R_a (I_2^2 - I_1^2), \quad (10)$$

where I_1 and I_2 are the currents under no load (without water in the tank) and loading conditions (with water) respectively. Similarly, the respective voltages are V_1 and V_2 , and R_a is the armature resistance.

As the impeller is located at the water surface, physical measurement of vortex depth is very difficult. Here the value for the vortex depth has been estimated using VISIMIX software. However, based on the visual observation the vortex depth was also measured at some speeds in order to validate the model result. It was determined by means of marks made on the shaft and tank wall corresponding to the initial liquid surface position. In cases where the vortex depth oscillated, the depth was estimated as the average between the upper and lower limits. Table 1 gives the range of all the parameters calculated either by experiment or through the software.

RESULTS AND DISCUSSION

Determination of critical radius and critical speed

A vortex generated in the tank follows the Rankine vortex distribution, and for each rotation there will be

Table 1 Ranges of parameter values.

Tank area (m ²)	Speed, <i>N</i> (rpm)	<i>K_La₂₀</i> (min ⁻¹)	Power consumption, <i>P</i> (W)	Mixing power, <i>P_{mixing}</i> (W)	Vortex depth, <i>V_d</i> (mm)
0.52	20–139	0.0102–1.07	0.67–30.8	0.0214–4.93	4–53
1.0	8–110	0.004–1.05	0.39–81.9	0.008–11.9	1.5–73

a critical radius of the forced vortex region. By using (3), the value of critical radius was obtained for each rotational speed (Fig. 2). Interestingly, it follows the Rankine distribution. The same observations can be seen in the experimental measurements also. Initially, a large interfacial vortex formed when the agitator started, drawing the upper water layer down into the impeller. This occurs up to the critical speed of the system (Fig. 2). According to Bernoulli's theorem, the pressure at the critical radius should be small or even be negative. This helps in sucking the air from the atmosphere in a surface aeration tank. As a consequence of this, the mass transfer coefficient (*K_La₂₀*) is larger at that point. That is why it is important to know about the critical radius and its characteristics. Critical speed is defined as the speed when the vortex reaches the impeller. Up to the critical speed, the vortex depth is proportional to Fr (Fig. 3). Above the critical speed, or when vortex reaches the impeller, the vortex depth becomes constant. But the critical radius starts decreasing and eventually becomes constant at high rotational speed. The value of the critical speed is 59.21 rpm in a big tank (critical radius 0.1486 m < rotor radius 0.175) and for the medium size tank, the value of critical radius is 71.85 rpm (critical radius 0.10672 m < rotor radius 0.125). There is a sharp

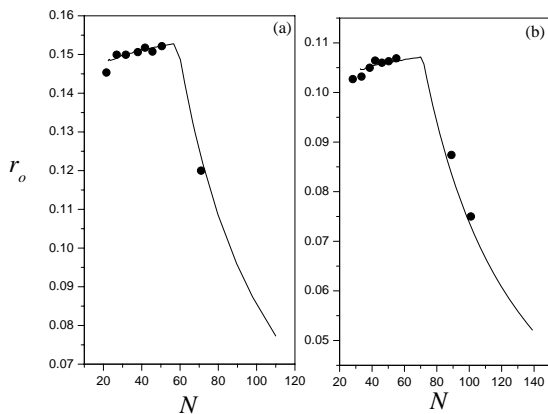


Fig. 2 Effect of rotational speed on critical radius. For this and subsequent figures, *A* = (a) 1.0 m² (b) 0.52 m². Squares: model; circles: experiment.

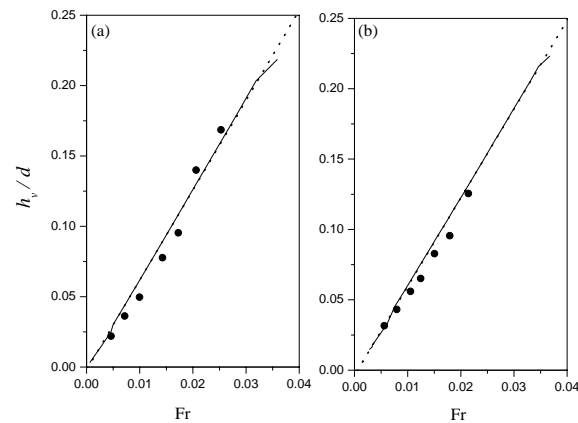


Fig. 3 Critical speed determination in surface aeration tanks.

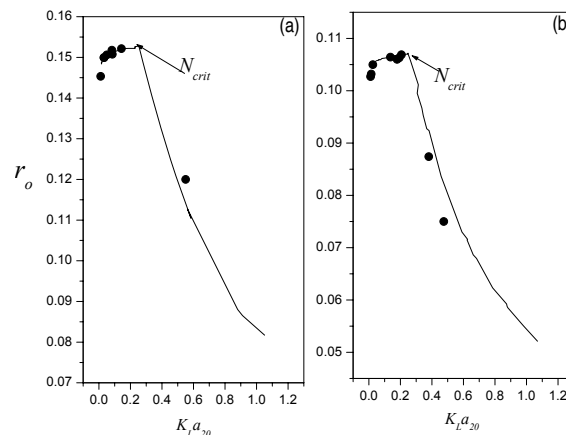


Fig. 4 Critical radius and mass transfer.

increase in the *K_La₂₀* near or above the critical speed (Fig. 4), which indicates the formation of a negative pressure zone. In this condition, air is being dragged into the tank. This increase in *K_La₂₀* can be attributed also to increased mixing power (Fig. 5). Initially, the power required for mixing increases gradually as the vortex depth increases. After reaching the critical speed, the vortex depth becomes constant but the power consumed for mixing increases sharply.

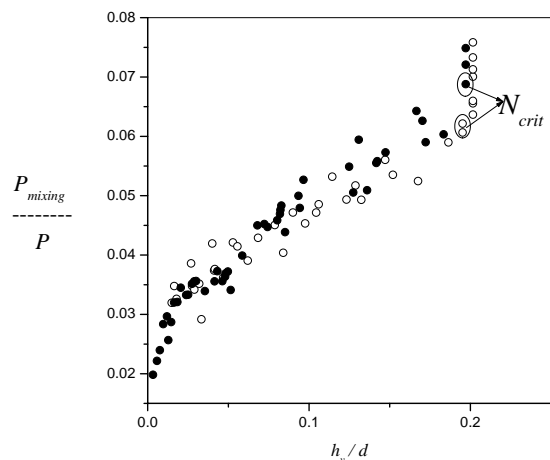


Fig. 5 Mixing power behaviour with vortex depth. In this figure and the next, filled squares: $A = 1.0 \text{ m}^2$; open squares: $A = 0.52 \text{ m}^2$.

Vortex depth correlation for surface aeration tank

If geometrical similarity is maintained, the dimensionless form of (8) is found to be suitable to scale up the process. Various researchers have given the formula to scale up the process characteristics. Here, the authors have adopted the formulas given by Zlokarnik¹⁹ and Rieger et al²⁰ for a six blade flat blade rotor and modified them to suit the present scenario. The scale-up criterion (Fig. 6) is given by

$$\frac{h_v}{d} = 43.2 \text{Fr}(0.1 - \text{Ga}^{-0.18})(H - h - b/d)^{-0.16} \quad (11)$$

$$\frac{h_v}{d} = 0.875 \text{Ga}^{0.069} \left(\frac{D}{d}\right)^{-1.18} \text{Fr}^{1.14} \text{Ga}^{-0.074} (D/d)^{0.14} \quad (12)$$

The modification in the earlier correlations is needed because of the differences in the type and configuration of the disk turbine used in the experiments. Experiments conducted by Reiger et al²⁰ and Zlokarnik¹⁹ have the rotor deep in the tank, whereas in the present experiments the rotor is placed near the water surface. The correlations developed in (11) and (12) are for geometrically similar systems. Based on the above correlations, scale-up or scale-down of the present results can be made for the commercial installation.

Acknowledgements: The financial support received through a research project from the Department of Science and Technology, New Delhi (Research Grant DSTO717) is gratefully acknowledged.

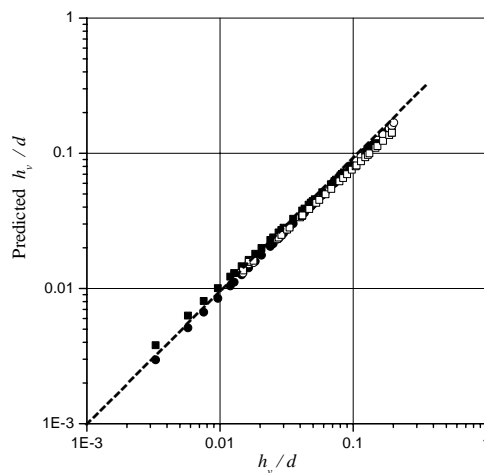


Fig. 6 Scale-up criterion based on vortex depth.

REFERENCES

- Reardon DJ (1995) Turning down the power. *Civ Eng* **65**, 54–6.
- Stenstrom MK, Vazirinejad HR, Ng AS (1984) Economic evaluation of upgrading aeration systems. *J WPCF* **56**, 20–6.
- Moucha T, Linek V, Prokopova E (2003) Gas hold-up, mixing time and gas–liquid volumetric mass transfer coefficient of various multi-impeller configurations: Rushton turbine, pitched blade and techmix impeller and their combinations. *Chem Eng Sci* **2**, 1839–46.
- Nienow AW (1998) Hydrodynamics of stirred bioreactors. *Appl Mech Rev* **51**, 1–32.
- Ozabek B, Gayik S (2001) The studies on the oxygen mass transfer coefficient in a bioreactor. *Process Biochem* **36**, 729–41.
- Rao ARK, Kumar Bimlesh (2007) The Use of Circular Surface Aerators in Wastewater Treatment Tanks. *J Chem Tech Biotechnol* **82**, 101–7.
- Smit L, During J (1991) Vortex geometry in stirred vessels. In: Proceedings of the 7th European Congress on Mixing, Bruges, Belgium, vol 2, pp 633–9.
- Markopoulos J, Kontogeorgaki E (1995) Vortex depth in unbaffled single and multiple impeller agitated vessels. *Chem Eng Tech* **18**, 68–74.
- Nagata S (1975) *Mixing: Principles and Applications*, Wiley, New York.
- Mazzarotta B (1993) Comminution phenomena in stirred sugar suspensions. *Am Inst Chem Eng Symp Ser* **89**, 112–7.
- Grisafi F, Brucato A, Rizzuti L (1994) Solid liquid mass transfer coefficients in mixing tanks: influence of side wall roughness. *Inst Chem Eng Symp Ser* **136**, 571–8.
- Glover GMC, Fitzpatrick JJ (2007) Modeling vortex formation in an unbaffled stirred tank reactor. *Chem Eng J* **127**, 11–22.

13. Middleton JC (1993) *Mixing in the Process Industries*, 2nd edn, Butterworths Heinemann, Oxford.
14. Ogawa A (1992) *Vortex flow*. CRC Press.
15. Ciofalo M, Brucato A, Grisafi F, Torrance N (1996) Turbulent flow in closed and free-surface unbaffled tanks stirred by radial impellers. *Chem Eng Sci* **51**, 3557–73.
16. Brennan DJ (1976) Vortex geometry in unbaffled vessels with impeller agitation. *Trans Inst Chem Eng* **54**, 209–17.
17. Tsao GTN (1968) Vortex behavior in the Waldhof fermentor. *Biotechnol Bioeng* **10**, 177–88.
18. van de Vusse JG (1955) Mixing by agitation of miscible liquids Part I. *Chem Eng Sci* **4**, 178–200.
19. Zlokarnik M (1971) Trombentiefe beim Rühren in unbewehrten Behältern. *Chem Ing Tech* **43**, 1028–30.
20. Rieger F, Ditzl P, Noval V (1979) Vortex depth in mixed unbaffled vessels. *Chem Eng Sci* **34**, 397–403.
21. Udaya SL, Sharma KVNS, Rao ARK (1991) Effect of geometrical parameters for overall oxygen transfer coefficient. In: *Proceedings of Symposium on Environmental Hydraulics*, Univ of Honkong, pp 1577–81.
22. Rao ARK, Kumar Bimlesh (2008) Scaling-up the geometrically similar unbaffled circular tank surface aerator. *Chem Eng Tech* **31**, 287–93.
23. Lewis WK, Whitman WG (1924) Principles of Gas Absorption. *Ind Eng Chem* **16**, 1215–20.
24. WEF, ASCE (1988) *Aeration: A waste water treatment process*, Water Environment Federation, Alexandria, and ASCE, New York.
25. Cook AL, Carr CC (1947) *Elements of Electrical Engineering*, 5th edn, Wiley, New York.